

Stochastic heart-rate model can reveal pathologic cardiac dynamics

Tom Kuusela*

Department of Physics, University of Turku, 20014 Turku, Finland

(Received 21 November 2003; published 31 March 2004)

A simple one-dimensional Langevin-type stochastic difference equation can simulate the heart-rate fluctuations in a time scale from minutes to hours. The model consists of a deterministic nonlinear part and a stochastic part typical of Gaussian noise, and both parts can be directly determined from measured heart-rate data. Data from healthy subjects typically exhibit the deterministic part with two or more stable fixed points. Studies of 15 congestive heart-failure subjects reveal that the deterministic part of pathologic heart dynamics has no clear stable fixed points. Direct simulations of the stochastic model for normal and pathologic cases can produce statistical parameters similar to those of real subjects. Results directly indicate that pathologic situations simplify the heart-rate control system.

DOI: 10.1103/PhysRevE.69.031916

PACS number(s): 87.19.Hh, 02.50.Ey

I. INTRODUCTION

Mathematical analyses of many physiological rhythms, including long-term heart-rate fluctuations, have shown that the underlying mechanisms are nonlinear, since linear systems cannot produce the observed complex behavior [1]. Nonlinear purely deterministic models can display chaotic dynamics and generate apparently unpredictable oscillations. However, in practice it has not yet been possible to extract such models directly from real experimental data [2]. Another possibility is that the underlying system is stochastic and that its time evolution is influenced by a noise source. There is also evidence that noise is an integral part of the dynamics of various biological systems [3–5], where this noise originates from the system itself or is a reflection of external influences.

Recently it has been shown that the long-term dynamics of the human heart rate can be modeled by a one-dimensional difference equation [6]:

$$X(t + \tau) = X(t) + g(X(t); \tau) + h(X(t); \tau)\Gamma(t), \quad (1)$$

where $X(t)$ represents the R - R interval at time t , τ is the time delay, function g gives the nonlinear deterministic change, and in the last term h is the amplitude of the stochastic contribution and $\Gamma(t)$ presents uncorrelated Gaussian noise with vanishing mean. In the limit $\tau \rightarrow 0$ [if $g(X(t); \tau)$ is approximated as $\tau g(X(t))$] we obtain the normal Langevin differential equation [7,8]. However, it has been shown that Eq. (1) is valid only if the delay parameter τ is in the range 2–20 min [6], since it is only within this range that the functions g and h do not depend significantly on the delay τ .

A simple method can be used to determine g and h from the measured time series [9,10]. First we divide the range of R - R intervals into equal-size bins. By scanning the whole time series we check when the R - R interval value is inside a bin, e.g., $|X(t_i) - x| \leq \Delta x$, where x is the middle value of the bin and Δx is the half width of the bin. When the value $X(t_i)$ occurs in the bin we look at the future value $X(t_i + \tau)$, where

τ is the fixed delay parameter. Since the trajectory of the system passes each bin several times, we can calculate the distribution of the future values for each bin. By assuming that the noise is Gaussian, we can fit a Gaussian function on each distribution. The mean of this distribution is equal to $X + g(X)$, and the deviation is equal to $h(X)$ [11,12]. When fitting the Gaussian function to the distribution we also calculated the correlation as $\sqrt{1 - S_{res}/S_{tot}}$ where S_{res} is the sum of the squared residuals and S_{tot} is the variance. The only values of $g(X)$ and $h(X)$ accepted were those associated with a correlation higher than 0.8.

In our analysis we have used R - R interval time series covering 22–24 h, corresponding to 80 000–100 000 data points. The data are actually interval data, i.e., they consist of a sequence of R - R interval values. Therefore it is more convenient to count the delay in terms of heart beats than seconds. Since the functions g and h are quite insensitive to the time delay, using a beat index as a variable does not significantly change their functional form [6]. The value of the delay parameter τ was 500 beats, and 100 bins were used to construct local distributions.

II. TYPICAL RESULTS FROM NORMAL AND HEART-FAILURE SUBJECTS

In order to discover if there are differences in the deterministic and stochastic parts of the model between normal and heart-failure subjects, we analyzed Holter recordings from 15 healthy subjects and from 15 patients with congestive heart failure (CHF; NYHA classification III or IV) of various ages and gender. The recordings are available in PhysioBank (MIT-BIH Normal Sinus Rhythm Database and BIDMC Congestive Heart Failure Database) [13]. The only recordings accepted were those with clear sinus rhythm and where the proportion of non-normal beats (mostly ventricular or supraventricular ectopic beats) was less than 5%.

In Fig. 1, we have presented typical R - R interval recordings of 80 min of healthy and CHF subjects. In the case of a normal subject (the upper panel) the variability of the R - R interval is larger and the mean interval clearly higher than in the case of a CHF subject (the lower panel). The short-time fluctuations of R - R interval of the normal subject are mostly

*Electronic address: tom.kuusela@utu.fi

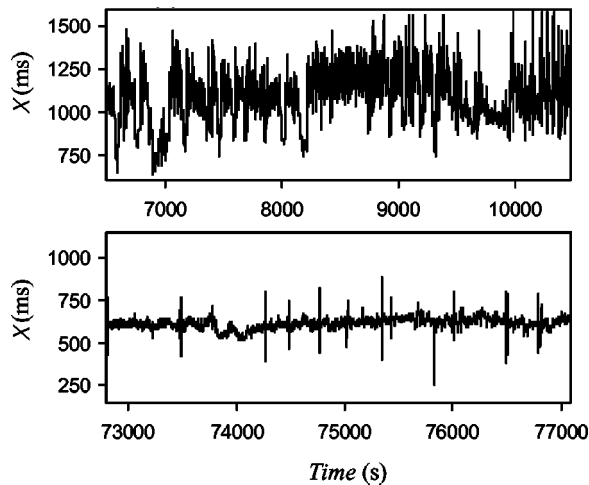


FIG. 1. Typical R - R interval time series of normal (upper panel) and heart-failure subjects.

generated by the respiration (periods normally couple of seconds) and blood pressure regulation (so called Mayer waves with periods of about 10 sec). These oscillations are rather small in the CHF subject. For normal subject large abrupt changes in the R - R interval are obvious but not evident for CHF case. Spikes in the R - R interval time series of the CHF subject are ectopic beats usually consisting of a pair of short and long beat.

Figure 2 presents typical analysis results obtained from a

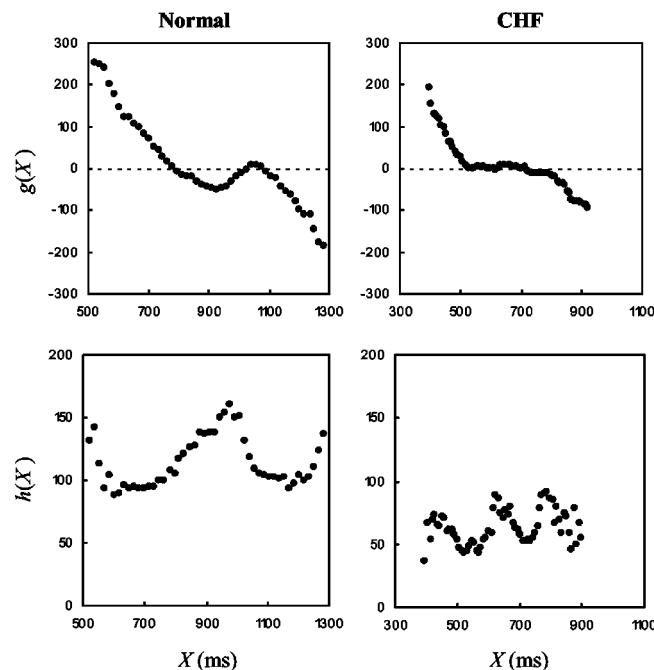


FIG. 2. Typical results derived from R - R interval time series for normal subjects (left panels) and CHF subjects (right panels), showing the deterministic part $g(X)$ (upper panels) and the stochastic part $h(X)$ (lower panels). In the normal case the deterministic part crosses the zero level three times: the first one and the last one are stable fixed points and the middle one is unstable. The deterministic part of the CHF subject exhibits no clear stable points.

healthy case and a CHF case. As reported previously [6], for healthy subjects it is most typical for the $g(X)$ function to cross the zero line three times, each representing a fixed point of the system, as shown in the top-left panel of Fig. 2. The left and right fixed points are stable: without any noise term these points attract all nearby states because the control function $g(X)$ is locally decreasing. In contrast, the middle fixed point is repulsive. This kind of “pitchfork” configuration of the fixed points is typical for systems exhibiting bistable behavior. The system has a tendency to jump between the stable points if the amplitude of the noise is sufficiently high. Far from the stable points the $g(X)$ function increases or decreases strongly, and this forces the system back to oscillate around stable points. It is possible for the $g(X)$ function to have more than three zeroes (but always an odd number thereof), indicating a multiple-pitchfork system [6]. In contrast, the deterministic part of the CHF case has no clear fixed points since the $g(X)$ function is practically zero and flat over a rather large range of R - R interval values, as can be seen in the top-right panel of Fig. 2. Again, at the lowest and highest values of the R - R interval the $g(X)$ function increases or decreases rapidly, forcing the system back to the flat part. However, within the flat part the system exhibits little control since there are no distinct stable fixed points—the system can wander freely.

The deterministic parts of a collection of CHF subjects are shown in Fig. 3. All of them have a clear flat segment, which distinguishes them from the pitchfork type of deterministic part of the normal subjects (see Fig. 5 in Ref. [6]). The length of the flat segment varies but in most cases it is around 200 ms, which represents a remarkably large part of the total range of the R - R interval, and hence the effect of this part on the dynamics of the system is not marginal. The mean level of the stochastic part $h(X)$ for normal subjects was 70–110 ms [6], and there was a maximum in $h(X)$ between the stable points, as evident in the example shown in the bottom-left panel of Fig. 2. The mean level of $h(X)$ was slightly less for CHF subjects, at 40–90 ms. Moreover, no obvious common structure was evident in $h(X)$, although sometimes the stochastic part appeared to have a complex structure, as can be seen in the example case in Fig. 2. The mean noise level, however, is large enough to force the system to explore also the rapidly increasing and decreasing parts of the $g(X)$ function.

CHF subjects normally exhibit considerably more ectopic beats (both ventricular and supraventricular) than normal subjects, and it is possible that these are totally or partially attributable to the form of the deterministic part. We therefore performed our analysis before and after editing out ectopic beats, as shown in Fig. 4. In this example of a CHF subject the total number of beats was 85 000, of which 1700 (2%) were classified as ectopic. All the ectopic beats were removed by the editing process. Figure 4 shows that the deterministic part $g(X)$ after editing (open dots) is practically identical to the original one (solid dots), from which we can conclude that the increased number of abnormal beats itself cannot explain the altered shape of the deterministic part for CHF subjects.

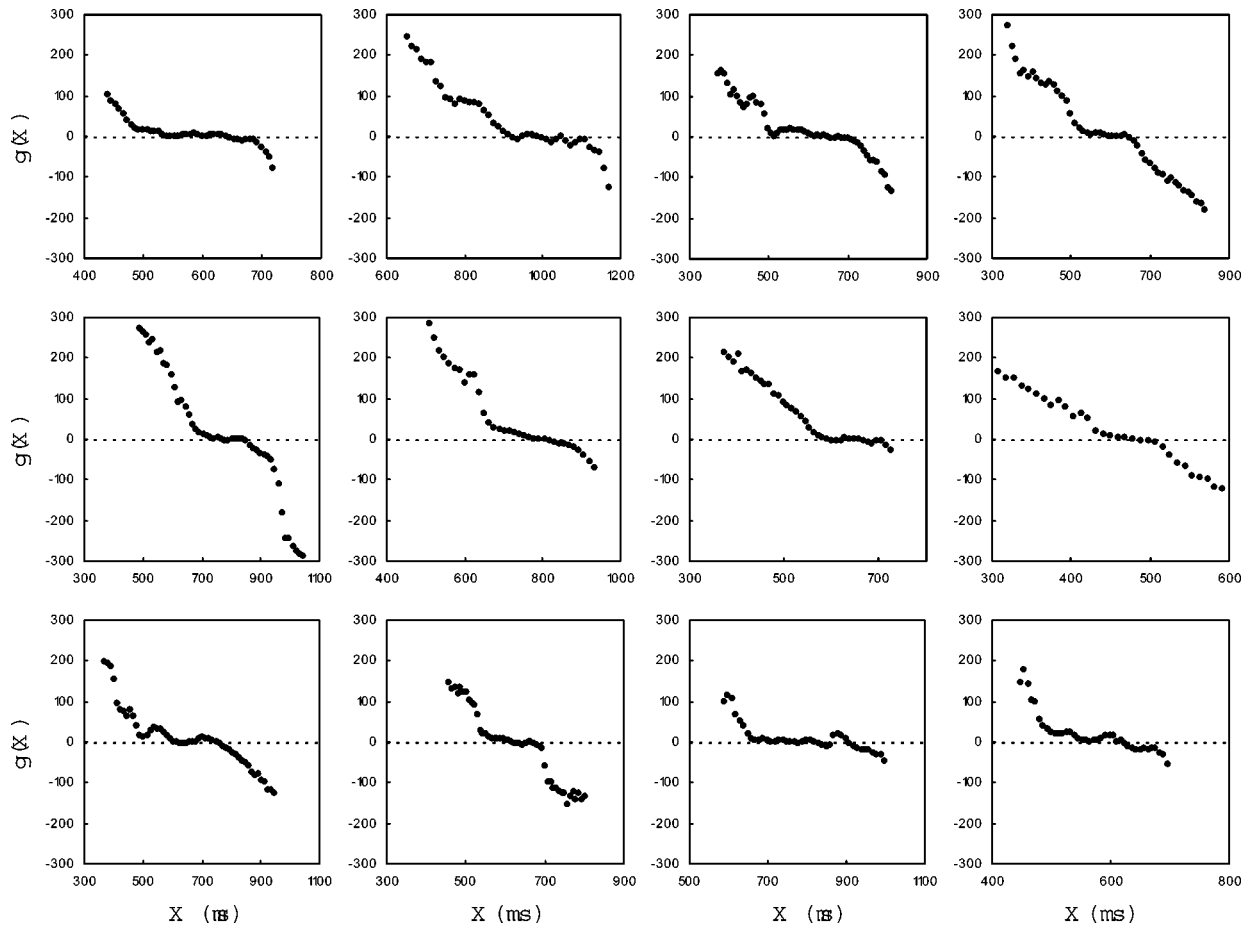


FIG. 3. Deterministic functions $g(X)$ derived from different CHF subjects. In all cases the functions exhibit a flat section near the zero line.

III. MODEL FOR NORMAL AND PATHOLOGIC DYNAMICS

We generated simulated time series in order to investigate the effects of different functional forms of the deterministic part of our stochastic model on various statistical parameters routinely used to analyze long-term heart-rate time series.

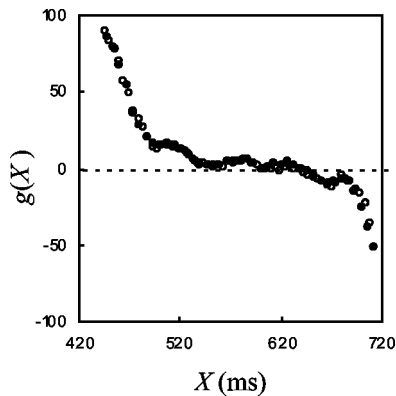


FIG. 4. The deterministic function $g(X)$ of one CHF subject before (solid dots) and after (open dots) editing out the ectopic beats. The deterministic function is practically unaltered by the editing process.

We used two forms of the control function $g(X)$: both were third-order polynomials but they had different coefficients. The function used to mimic normal subjects has two stable fixed points and one unstable one, as shown in the left panel of Fig. 5. Also, the heights of the local minima and maxima

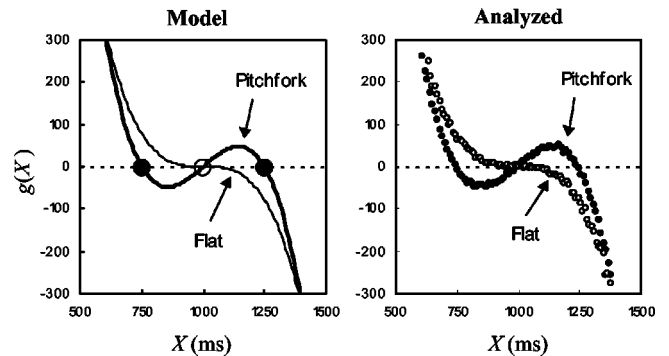


FIG. 5. Left panel shows the model functions used in simulations. The “pitchfork” type of deterministic function $g(X)$ has two stable fixed points (solid dots) and one unstable point (open dot), whereas the “flat” type of function exhibits only one unstable point. The deterministic parts derived from the simulated time series using pitchfork and flat model functions closely resemble the original ones (right panel).

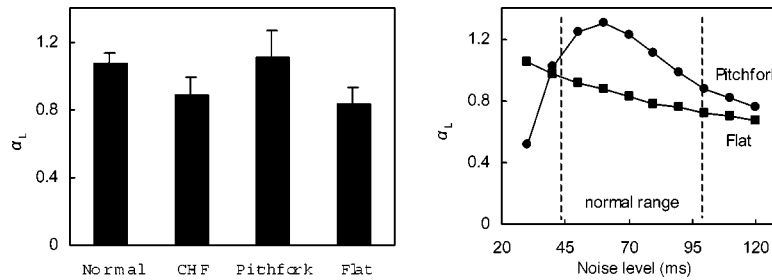


FIG. 6. The long-range scaling exponent α_L calculated by DFA for normal and CHF subjects, and from the simulated time series using the pitchfork and flat deterministic functions (left panel). Results are shown as means and standard deviations for 15 subjects or simulations. The right panel shows the scaling exponent as a function of the noise level used in simulations with pitchfork and flat deterministic functions. The normal range of the noise level (marked with dashed vertical lines) corresponds to mean levels of the stochastic parts found in real subjects.

were adjusted to resemble the typical features of the function $g(X)$ extracted from real normal subjects. The model function simulating CHF subjects has no local minima or maxima; it instead has a flat segment near the zero line (we call this function “flat”). It should be noticed that both types of model functions are centered on an R - R interval of 1000 ms. In the case of CHF subjects the mean R - R interval is normally much shorter, but since we are not interested in absolute values of the R - R interval (which our model cannot predict) but merely in the variability and complexity of the time series, this choice does not affect our results. For the stochastic part $h(X)$ we simply used a constant value since we could not identify any common features in this part, especially in CHF subjects.

In simulations we used the difference equation (1) to directly compute the R - R interval time series. Since the model is based on analyses from real data with the delay parameter value of 500 beats, the simulated time series is not a beat-to-beat series—instead, the time variable (or index) is in units of 500 beats. To check that our approach is self-consistent we analyzed the simulated time series (now with a time delay of 1); the results are shown in the right panel of Fig. 5. The extracted deterministic parts $g(X)$ for the pitchfork and flat types of model function closely resemble the original ones.

IV. STATISTICAL ANALYSIS OF REAL AND SIMULATED DATA

A. Detrended fluctuation analysis

Detrended fluctuation analysis (DFA) is widely used to characterize the long-range correlation behavior of R - R interval time series [14,15]. DFA can be used to quantify self-similar properties of a signal. In the case of the R - R interval the power-law scaling exponent of DFA is normally determined in two regions: (1) the short-range scaling exponent α_S covers the time range from 0 to 10 sec (or beats), and (2) the long-range scaling exponent α_L covers from 10 sec to tens of minutes or even hours. For totally uncorrelated signals (e.g., white noise) the scaling exponent takes the value 0.5, $1/f$ noise has a value of 1.0, and Brownian noise (the integral of white noise or random walking) has the value 1.5. Since our stochastic model cannot cover correlations shorter than the time delay (500 beats in our analysis), we are inter-

ested only in α_L . We calculated α_L for our database of normal and CHF subjects, and the results are shown in the left panel of Fig. 6. Typically α_L is close to one in the case of a healthy subject, as we also found ($\alpha_L = 1.08 \pm 0.06$, mean \pm SD). For CHF subjects the results in the literature are more diverse. It has been reported that α_L increases in pathologic situations, but in practice the situation is more variable (e.g., see Ref. [15]: the range of α_L values for normal subjects was 0.7–1.2 and for CHF subjects was 0.6–1.5 with a rather flat distribution; and hence the change in the mean values of α_L does not describe the real effect very well). In our CHF database α_L was 0.88 ± 0.09 , which is significantly lower than that in normal subjects ($p \leq 0.001$ by t -test for independent samples).

To compare the scaling properties of the simulated time series with the real ones we generated time series using pitchfork and flat model functions for several different noise levels. The range of the noise level, 40–100 ms, was approximately the same as that found from the analysis of real subjects. The mean values of α_L over these 15 different simulations are also shown in the left panel of Fig. 6. Interestingly, the mean α_L from simulations with the pitchfork control function is very close to that of normal subjects, and simulations with the flat function are close to those for CHF subjects. α_L is plotted as a function of the noise level in the right panel of Fig. 6. Within the noise range of 40–120 ms the pitchfork model gives clearly higher α_L values than the flat model. However, if the noise amplitude is very low, α_L of the pitchfork model drops since the system can no longer jump between the stable points—it instead merely oscillates around one point. With large noise levels both models give almost equal α_L values, and the details of the deterministic function $g(X)$ are no longer important.

B. Spectral power

It is well known that the total variability of the heart rate is significantly lower in CHF subjects. We calculated the spectral power of the real and simulated R - R interval time series over the lowest frequency bands—ultralow frequency (ULF) band (0–0.003 Hz) and very low frequency (VLF) band (0.003–0.04 Hz)—using fast Fourier transformation (as explained earlier, our model cannot explain faster oscillations).

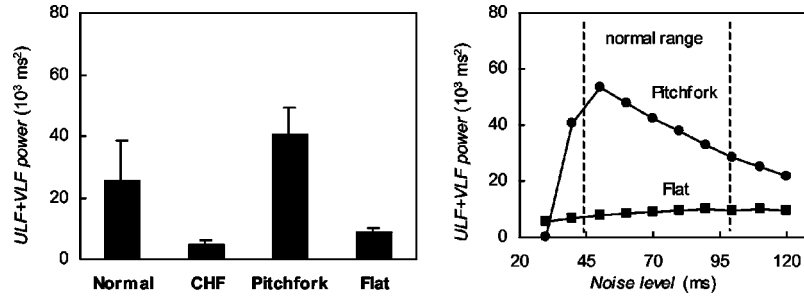


FIG. 7. The spectral power in ULF and VLF frequency bands for normal and CHF subjects, and from the simulated time series using the pitchfork and flat deterministic functions (left panel). Results are shown as means and standard deviations for 15 subjects or simulations. The right panel shows the spectral power as a function of the noise level used in simulations with pitchfork and flat deterministic functions.

tions). The results averaged over 15 real normal and CHF subjects, and 15 pitchfork and flat types of simulation are presented in the left panel of Fig. 7. Again the pitchfork system closely resembles normal subjects, and the flat system resembles CHF subjects. The spectral power as a function of the noise level is displayed in the right panel of Fig. 7. It is remarkable that with the same level of noise the power of the pitchfork system is several-fold that of the flat system, with a maximum at a noise level of 50 ms. In contrast, the spectral power of the flat system is quite insensitive to the noise amplitude.

C. Multifractal analysis

It has been shown previously that the time series of healthy human *R-R* intervals exhibits multifractal properties [16,17]. Monofractal signals can be indexed by a single global Hurst exponent [18], whereas multifractal signals can be decomposed into many subsets characterized by different local Hurst exponents *h* which quantify the local singular behavior related to the local fractal properties of the time series [19]. The statistical properties of the different subsets can be quantified by the singularity spectrum *D(h)*, which is the fractal dimension of the subset as a function of the local Hurst exponent. Monofractal signals exhibit a narrow range of *h* values, whereas for multifractal signals the function *D(h)* is broad.

We calculated the singularity spectrum in the following manner [20]. First we constructed the *L*¹-norm wavelet transform of the *R-R* interval time series

$$WT(a,t) = \frac{1}{a} \int_{-\infty}^{\infty} X(t') \Psi\left(\frac{t'-t}{a}\right) dt', \quad (2)$$

where the $\Psi(t)$ is the wavelet analysis function. We used the second derivative of the Gaussian function as an analysis function. The next phase involved detection of the local maxima *t_k* of the modulus $|WT(a,t)|$ at a given scale *a*. The partition function is the sum of the *q* moments of the wavelet transform modulus over the local maxima,

$$Z(a,q) = \sum_{\{t_k(a)\}} |WT(a,t_k(a))|^q. \quad (3)$$

For small scales, we can assume that [20]

$$Z(a,q) \approx a^{l(q)}. \quad (4)$$

In practice, *l(q)* can be determined by plotting $\ln[Z(a,q)]$ as a function of $\ln(a)$ and fitting a straight line over suitable range of *a* values; the slope of the line gives *l(q)*. We calculated *l(q)* for moments *q* = -5 to 5, and obtained the slope in the region 20 ≤ *a* ≤ 500. The singularity spectrum is given from *l(q)* through the Legendre transform

$$D(h) = q \frac{dl(q)}{dq} - l(q). \quad (5)$$

The results from this multifractal analysis of the simulated time series are shown in Fig. 8. At a noise level of 60 ms, *D(h)* from the pitchfork system (solid dots, the curve labeled 60) has nonzero values for a broad range of the local Hurst exponents, with the maximum at *h* = 0.16 indicating the actual multifractal behavior of the system. These kind of fractal dimensions have been observed in healthy subjects: the maximum of *D(h)* has been found to be 0.14 ± 0.04 and the width of the *D(h)* spectrum 0.16 [16,17]. If 0 ≤ *h* ≤ 0.5 the fluctuations in the *R-R* interval dynamics exhibit anticorrelated behavior, as reported several times in the case of

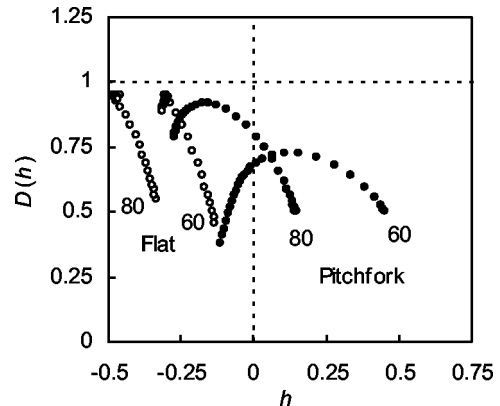


FIG. 8. The fractal dimension *D(h)* as a function of the Hurst exponent *h* derived from the simulated time series using pitchfork (solid dots) and flat (open dots) deterministic functions. Two noise levels were used in the simulations: 60 and 80 ms.

healthy subjects ($h=0$ corresponds to $1/f$ behavior, $h=0.5$ to random walking, and $h>0.5$ to correlated behavior). Since for monofractal signals the Hurst exponent h and the scaling exponent α_L from DFA are related by the equation $h=\alpha_L-1$, we can see that our result from DFA is consistent with multifractal analysis; it should be noticed that for real multifractal signals we can approximately relate the Hurst exponent corresponding to the maximum of $D(h)$ and the scaling exponent α_L . If the noise level is increased to 80 ms (solid dots in Fig. 8, the curve labeled “80”), the maximum of the $D(h)$ is shifted to the left and the corresponding Hurst exponent is slightly negative but the singular spectrum is still rather wide.

When using the flat type of control function in simulations, the $D(h)$ spectrum is narrow and the maximum is found on a negative Hurst exponent (see Fig. 8, curves with open dots). For totally uncorrelated white noise the local Hurst exponent is -0.5 , and at a noise level of 80 ms the system almost reaches this situation. With both levels of noise the flat control function produces an almost monofractal signal. In previous studies it has been observed that the statistically dominant Hurst exponents for heart-failure subjects are confined to a narrower range, as we have found with the flat control function; but, in contrast, the maximum of $D(h)$ shifts towards higher h values indicating that fluctuations in $R-R$ interval are less anticorrelated (and more like random walking) [16]. However, our observations based on multifractal analysis are consistent with our DFA results: the mean α_L of CHF subjects from our database is clearly less than 1.0, corresponding to negative Hurst exponents, and the system dynamics produces a signal that is indistinguishable from white noise. It is therefore obvious that different CHF databases can produce apparently contradictory findings, as we have discussed already in the context of DFA.

V. CONCLUSION

We have shown that a one-dimensional stochastic difference equation can explain some fundamental features of nor-

mal and pathologic heart-rate dynamics. Our model cannot predict beat-to-beat oscillations of the $R-R$ interval but it can simulate long-term behavior up to delays of 500 beats. Our observations indicate that uncorrelated Gaussian noise—originating either from the system itself or externally—can produce complex and even multifractal behavior when affecting the system through a simple but nonlinear control function, the deterministic part of the model. If the control function has a pitchfork configuration (i.e., two stable fixed points and one unstable one), the system produces a time series that resembles the dynamical properties of the heart rate of normal healthy subjects, at least when comparing some fundamental statistical parameters used to characterize heart-rate dynamics. Surprisingly the control function of a heart-failure subject has no clear stable points, which allows the system to wander rather freely. It has been suggested that certain real pathologic situations simplify the heart-rate control system by weakening or completely removing some of the feedback loops, and the resulting time series behaves more like a random walk. Our stochastic model supports this idea, since the control function of CHF subjects lack all complex features. In contrast, our model predicts that the pathologic dynamics produces white-noise-like behavior, and not random walking. However, variations in DFA measurements of pathologic data suggest that the underlying clinical conditions vary among heart-failure patients, and our model can perhaps cover only part of them. We found that in some cases the stochastic part can have a rather complex structure, and it is possible that a more complicated stochastic part would produce different dynamics. In summary, we can conclude that distinguishing the shapes of the deterministic parts of the $R-R$ interval time series of normal and heart-failure subjects provides a diagnostic tool for the prediction of some pathologic conditions.

ACKNOWLEDGMENT

This work was supported by the Academy of Finland.

-
- [1] L. Glass, *Nature (London)* **410**, 277 (2001).
 - [2] L. Glass and M. C. Mackey, *From Clocks to Chaos: The Rhythms of Life* (Princeton Univ. Press, Princeton, 1988).
 - [3] J.J. Collins, T.T. Imhoff, and P. Grigg, *J. Neurophysiol.* **76**, 642 (1996).
 - [4] I. Hidaka, D. Nozaki, and Y. Yamamoto, *Phys. Rev. Lett.* **85**, 3740 (2000).
 - [5] D.J. Mar, C.C. Chow, W. Gerstner, R.W. Adams, and J.J. Collins, *Proc. Natl. Acad. Sci. U.S.A.* **96**, 10450 (1999).
 - [6] T.A. Kuusela, T. Shepherd, and J. Hietarinta, *Phys. Rev. E* **67**, 061904 (2003).
 - [7] N.G. van Kampen, *Stochastic Processes in Physics and Chemistry* (North-Holland, New York, 1981).
 - [8] H. Risken, *The Fokker-Planck Equation* (Springer, Berlin, 1984).
 - [9] J. Gradišek, S. Siebert, R. Friedrich, and I. Grabec, *Phys. Rev. E* **62**, 3146 (2000).
 - [10] S. Siebert, R. Friedrich, and J. Peinke, *Phys. Lett. A* **243**, 275 (1998).
 - [11] J. Timmer, *Chaos, Solitons Fractals* **11**, 2571 (2000).
 - [12] R. Friedrich, S. Siebert, J. Peinke, St. Lück, M. Siefert, M. Lindeman, J. Raethjen, G. Deuschl, and G. Pfister, *Phys. Lett. A* **271**, 217 (2000).
 - [13] A.L. Goldberger, L.A.N. Amaral, L. Glass, J.M. Hausdorff, P.Ch. Ivanov, R.G. Mark, J.E. Mietus, G.B. Moody, C.K. Peng, and H.E. Stanley, *Circulation* **101**, e215 (2000).
 - [14] N. Iyengar, C.-K. Peng, R. Morin, A.L. Goldberger, and L.A. Lipsitz, *Am. J. Physiol.* **271**, R1078 (1996).
 - [15] C.-K. Peng, S. Havlin, H.E. Stanley, and A.L. Goldberger, *Chaos* **5**, 82 (1995).

- [16] P.Ch. Ivanov, L.A.N. Amaral, A.L. Goldberger, S. Havlin, M.G. Rosenblum, Z.R. Struzik, and H.E. Stanley, *Nature (London)* **399**, 461 (1999).
- [17] L.A.N. Amaral, P.Ch. Ivanov, N. Aoyagi, I. Hidaka, S. Tomono, A.L. Goldberger, H.E. Stanley, and Y. Yamamoto, *Phys. Rev. Lett.* **86**, 6026 (2001).
- [18] H.E. Hurst, *Trans. Am. Soc. Civ. Eng.* **116**, 770 (1951).
- [19] T. Vicsek and A.L. Barabasi, *J. Phys. A* **24**, L845 (1991).
- [20] J.F. Muzy, E. Bacry, and A. Arneodo, *Phys. Rev. Lett.* **67**, 3515 (1991).